



## Cotransport of clay colloids and viruses through water-saturated vertically oriented columns packed with glass beads: Gravity effects



Vasiliki I. Syngouna<sup>a</sup>, Constantinos V. Chrysikopoulos<sup>b,\*</sup>

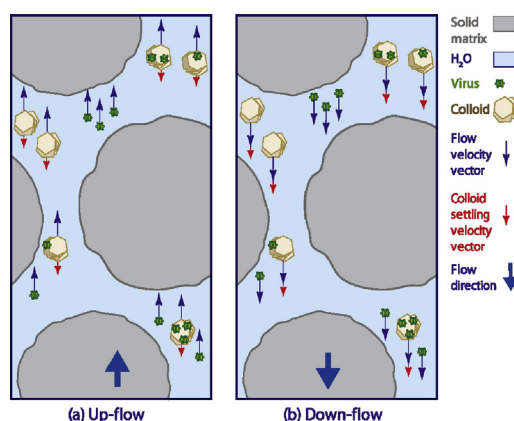
<sup>a</sup> Environmental Engineering Laboratory, Civil Engineering Department, University of Patras, Patras 26500, Greece

<sup>b</sup> School of Environmental Engineering, Technical University of Crete, Chania 73100, Greece

### HIGHLIGHTS

- Gravity affects viruses and clay colloids cotransport in porous media.
- Colloids can facilitate or hinder the transport of viruses in porous media.
- Virus attachment in the presence of colloids is greater for up-flow than down-flow.

### GRAPHICAL ABSTRACT



### ARTICLE INFO

#### Article history:

Received 8 October 2015

Received in revised form 27 November 2015

Accepted 19 December 2015

Available online xxxx

Editor: D. Barcelo

#### Keywords:

Gravity effects

ΦX174

MS2

Clay minerals

KGa-1b

STx-1b

Viruses

Colloids

Cotransport

Porous media

### ABSTRACT

The cotransport of clay colloids and viruses in vertically oriented laboratory columns packed with glass beads was investigated. Bacteriophages MS2 and ΦX174 were used as model viruses, and kaolinite (KGa-1b) and montmorillonite (STx-1b) as model clay colloids. A steady flow rate of  $Q = 1.5$  mL/min was applied in both vertical up (VU) and vertical down (VD) flow directions. In the presence of KGa-1b, estimated mass recovery values for both viruses were higher for VD than VU flow direction, while in the presence of STx-1b the opposite was observed. However, for all cases examined, the produced mass of viruses attached onto suspended clay particles were higher for VD than VU flow direction, suggesting that the flow direction significantly influences virus attachment onto clays, as well as packed column retention of viruses attached onto suspended clays. KGa-1b hindered the transport of ΦX174 under VD flow, while STx-1b facilitated the transport of ΦX174 under both VU and VD flow directions. Moreover, KGa-1b and STx-1b facilitated the transport of MS2 in most of the cases examined except of the case where KGa-1b was present under VD flow. Also, the experimental data were used for the estimation of virus surface-coverages and virus surface concentrations generated by virus diffusion-limited attachment, as well as virus attachment due to sedimentation. Both sedimentation and diffusion limited virus attachment were higher for VD than VU flow, except the case of MS2 and STx-1b cotransport. The diffusion-limited attachment was higher for MS2 than ΦX174 for all cases examined.

© 2015 Elsevier B.V. All rights reserved.

\* Corresponding author.

E-mail address: [cvc@enveng.tuc.gr](mailto:cvc@enveng.tuc.gr) (C.V. Chrysikopoulos).

## 1. Introduction

Numerous experimental and theoretical studies published in the literature have focused on factors that govern colloid and biocolloid (e.g. viruses, bacteria) transport in fractured and porous media (Zhuang and Jin, 2003; Bradford et al., 2006; Torkzaban et al., 2007; Kim et al., 2009; Chrysikopoulos et al., 2010, 2012; Syngouna and Chrysikopoulos, 2015; Sen, 2011; Shen et al., 2012; Katzourakis and Chrysikopoulos, 2014, 2015; Seetha et al., 2015; Kokkinos et al., 2015), have examined the role of velocity on colloid transport and deposition, in conjunction with the influence of either the particle size (e.g. Bradford et al., 2006; Chrysikopoulos and Katzourakis, 2015), or the ionic strength (e.g., Tong et al., 2008; Tosco et al., 2009; Mitropoulou et al., 2013; Torkzaban et al., 2015). Other factors that have been evaluated include the role of roughness and flow direction (Yoon et al., 2006; Bradford and Torkzaban, 2013), collector size (Xu et al., 2006; Syngouna and Chrysikopoulos, 2011), pore geometry or grain angularity (Tong and Johnson, 2006; Ma and Johnson, 2010), and chemical heterogeneity of the porous media (Bradford and Torkzaban, 2012). Moreover, the presence of colloids suspended in the aqueous phase has been shown to either enhance or hinder the transport of organic and inorganic pollutants (Kretzschmar et al., 1999; Walshe et al., 2010; Syngouna and Chrysikopoulos, 2013).

The effect of flow direction on colloid and biocolloid transport in porous media has received relatively minor attention (Ma et al., 2009; Chrysikopoulos and Syngouna, 2014). The flow direction employed in typical contaminant transport experimental investigations is horizontal (Silliman et al., 2001; Syngouna and Chrysikopoulos, 2011, 2013; Vasiliadou and Chrysikopoulos, 2011), downward (Anders and Chrysikopoulos, 2009; Chrysikopoulos et al., 2010; Xu et al., 2006), or upward (Bradford et al., 2006; Tong and Johnson, 2007). The upward flow direction is often selected in order to minimize air entrapment. Previous experimental observations have revealed that flow direction influences colloid transport in porous media showing greater rate of particle deposition for up-flow than for down-flow direction and suggesting that gravity was a significant driving force for colloid deposition (Chrysikopoulos and Syngouna, 2014). However, the effect of flow direction on the cotransport of clay colloids and viruses has not been previously explored.

The present study examined the effect of flow direction on the cotransport of clay colloids and viruses in vertical water-saturated columns packed with glass beads. A steady flow rate was applied in both vertical up (VU) and vertical down (VD) directions. Bench scale experiments were performed to investigate the interactions between viruses and clays during their simultaneous transport (cotransport) in porous media. Also the synergistic effects of suspended clay colloids and flow direction on the attenuation and transport of viruses in porous media was examined. Furthermore, virus diffusion-limited attachment and virus attachment by sedimentation were evaluated for all the cotransport experiments conducted in this study.

## 2. Materials and methods

### 2.1. Bacteriophages and assay

The bacteriophage MS2 (F-specific single-stranded RNA phage with effective particle diameter ranging from 24 to 26 nm) has been recommended as a surrogate for poliovirus due to similarities in size, and has been employed as a conservative tracer for enteric virus transport, because MS2 attachment onto the majority of soil types is low compared to many other viruses (Jin and Flury, 2002; Schjiven et al., 1999). Moreover, the bacteriophage  $\Phi$ X174 (somatic single-stranded DNA phage with effective particle diameter ranging from 25 to 27 nm) has been recommended as an indicator for enteric viral pathogens (Gantzer et al., 1998). Both bacteriophages are infecting *Escherichia coli*, and were

assayed by the double-layer overlay method (Adams, 1959), as outlined by Syngouna and Chrysikopoulos (2011).

Each initial virus concentration used in this study, collected from the same virus stock solution was diluted with sterile distilled deionized water (ddH<sub>2</sub>O), which was purified with a Milli-Q UV plus water purification system (Millipore Corp., Massachusetts). The resulting viral suspension was close to neutral. For the separation of viruses attached onto clay colloids from suspended viruses in the liquid phase, 0.3 mL of the density gradient separation reagent Histodenz (60% by weight, Axis-Shield PoC AS Company, Norway) was added to 2 mL of the liquid sample (Vasiliadou and Chrysikopoulos, 2011; Jiang et al., 2007; Rong et al., 2008), the mixture was centrifuged at 2000×g for 30 min so that the supernatant was free of clay colloids.

The suspension of unattached viruses in the supernatant was pipetted out and the suspended viruses were determined. The absence of clay colloids in the supernatant was verified by a UV–vis spectrophotometer (UV-1100, Hitachi) at a wavelength of 280 nm. The concentration of attached viruses was determined by subtracting the mass of viruses that remained in suspension from the initial virus concentration in each sample. Because only viable viruses were measured in the water samples, it was important to exclude the effect of virus inactivation when evaluating interactions of viruses with clay colloids under the present experimental conditions. Previous batch inactivation experiments under identical experimental conditions, in the presence and absence of clays, suggested that no significant virus inactivation is expected during the experimental time period (Chrysikopoulos and Syngouna, 2012; Bellou et al., 2015). Although the inactivation rates of the viruses used in this study are relatively small, MS2 inactivation rate of  $4.2 \times 10^{-5} \text{ min}^{-1}$  was reported to be more than two times larger than  $2.0 \times 10^{-5} \text{ min}^{-1}$  that of  $\Phi$ X174 (Syngouna and Chrysikopoulos, 2011). Furthermore, the inactivation rate of MS2 was reported to be greater than that of  $\Phi$ X174 in the presence of quartz sand under static and dynamic batch conditions at different temperatures (Chrysikopoulos and Aravantinou, 2012). Therefore, the difference in the inactivation rate coefficients between MS2 and  $\Phi$ X174 is expected to yield smaller MS2 breakthrough concentrations than  $\Phi$ X174. Note that inactivation of suspended viruses in water saturated porous media is controlled by the physicochemical characteristics of viruses (Yamagishi and Ozeki, 1972), formation temperature (Yates and Yates, 1988), and time (Sim and Chrysikopoulos, 1996; Anders and Chrysikopoulos, 2006). Certainly, the inactivation rates of liquid-phase and attached viruses should not be assumed equal (Chrysikopoulos and Sim, 1996; Sim and Chrysikopoulos, 1999). Moreover, inactivation of clay-attached viruses can either be enhanced due to distortion and unfolding of protein structure caused by strong electrostatic attraction, or reduced due to virus protection provided by the clay particles (Schjiven and Hassanizadeh, 2000; Ryan et al., 2002).

### 2.2. Clays

The clays used in this study were kaolinite (KGa-1b, well-crystallized kaolin, from Washington County, Georgia) (Pruett and Webb, 1993), and montmorillonite (STx-1b, Ca-rich montmorillonite, Gonzales County, Texas), purchased from the Clay Minerals Society (Columbia, USA). KGa-1b has specific surface area (SSA) of 10.1 m<sup>2</sup>/g, as evaluated by the Brunauer–Emmet–Teller (BET) method, and cation exchange capacity (CEC) of 2.0 meq/100 g (van Olphen and Fripiat, 1979). STx-1b has a SSA of 82.9 m<sup>2</sup>/g (Sanders et al., 2010), and assuming that the characteristics of STx-1b are comparable to those of STx-1, which is the previous batch of montmorillonite from the same area, its CEC is 84.4 meq/100 g (van Olphen and Fripiat, 1979). The <2 μm colloidal fraction, used in the transport experiments, was separated by sedimentation and was purified following the procedure described by Rong et al. (2008). It should be noted that the treated clays (purified colloidal fraction) are smaller than the untreated particles, and thus is reasonable to assume that the treated clays are expected to have higher SSA values

than the untreated particles. The viral and clay colloidal suspensions prepared in high purified sterile ddH<sub>2</sub>O, ensuring that the pH is close to neutral. The average intensity-weighted hydrodynamic diameter ( $\pm$ SD between three replicates) of the clay colloids was measured by a zetasizer (Nano ZS90, Malvern Instruments) and was found to be equal to  $d_p = 842.85 \pm 125.85$  nm for KGa-1b, and  $d_p = 1187 \pm 380.81$  nm for STx-1b, resulting in a virus-to-clay particle size ratio in the range from 0.026 to 0.036 for KGa-1b particles, and from 0.016 to 0.032 for STx-1b particles. Also, the polydispersity index (PDI) was  $<0.3$  for KGa-1b and  $<0.5$  for STx-1b, calculated by a cumulants analysis of the intensity autocorrelation function measured by dynamic light scattering (DLS). The optical density of the clay colloids was analyzed at a wavelength of 280 nm by a UV–vis spectrophotometer, and the corresponding clay concentrations were determined by the procedures outlined by Chrysikopoulos and Syngouna (2012).

### 3. Column experiments

All of the cotransport experiments were conducted in 30-cm long Chromaflex glass columns with 2.5 cm inside diameter packed with 2 mm in diameter glass beads (Fisher Scientific, New Jersey). Glass beads were chosen as model porous media because they are chemically non-reactive with the solutions used in this study. Prior to the experiments, the beads were cleaned with 0.1 M HCl for 3 h to remove surface impurities (e.g. iron hydroxide and organic coatings) that could promote physicochemical deposition of colloids, rinsed with ddH<sub>2</sub>O, then soaked in 0.1 M NaOH for 3 h and rinsed with ddH<sub>2</sub>O again. After the cleaning steps, the beads were dried in an oven at 105 °C and then stored in screw cap sterile beakers until use in the column experiments.

The column was placed vertically and packed with glass beads under standing sterile ddH<sub>2</sub>O (pH 7,  $I_s = 10^{-4}$  M) to minimize air entrapment. The estimated dry bulk density was 1.61 g/cm<sup>3</sup>, and the porosity was 0.42. Also, 3 pore volumes (PV) of sterile ddH<sub>2</sub>O were passed through the column prior to each flowthrough experiment. The entire packed column as well as all the glassware and materials used for the experiments were sterilized in an autoclave at 121 °C for 20 min. Constant flow of sterile ddH<sub>2</sub>O at a flow rate of  $Q = 1.5$  mL/min, corresponding to interstitial water velocity of  $U = 0.74$  cm/min, was applied in both vertical up (VU) and vertical down (VD) flow directions through the packed column with a peristaltic pump. A fresh column was packed for each experiment. Flowthrough experiments were performed with the viral suspension and the clay colloidal suspension injected simultaneously into the vertically oriented packed column. The constant influent (initial) virus,  $C_{v0}$  [M/L<sup>3</sup>] and clay,  $C_{c0}$  [M/L<sup>3</sup>] concentrations were equal to  $3.7 \pm 0.9 \times 10^3$  PFU/mL,  $11.6 \pm 4.4 \times 10^3$  PFU/mL,  $80.4 \pm 9.4$  mg/L and  $113.2 \pm 14.4$  mg/L for  $\phi$ X174, MS2, KGa-1b and STx-1b, respectively. These clay colloid concentrations are similar to those used in other laboratory transport studies (Gao et al., 2004). It should also be noted that virus concentrations range from 10 to 10<sup>7</sup> PFU/mL in sewage waters (Snowdon et al., 1989). Colloid concentrations range from less than 1 mg/L to several hundred mg/L in subsurface formations (Moulin and Ouzounian, 1992; Degueldre et al., 1996). Mobile colloids are omnipresent in unsaturated subsurface formations (vadose zone), where during rainfall may reach concentrations up to 1000 mg/L (DeNovio et al., 2004). In general, there are fewer colloids present in deeper aquifers than in shallower subsurface formations.

For the virus and clay colloid cotransport experiments, 3 PVs of both suspensions were injected into the packed column, followed by 3 PVs of ddH<sub>2</sub>O. The nonreactive tracer (chloride) breakthrough experiments were performed by injecting 3 PVs of 0.01 M KCl into the column, followed by 3 PV of ddH<sub>2</sub>O (data not shown). It should be noted that alkali halides are the most commonly used salts for subsurface fluid tracing owing to a minimal effect on solution ionic strength. Chloride concentrations were measured using ion chromatography (ICS-1500, Dionex Corp., Sunnyvale, CA). All experiments were carried out at room temperature ( $\sim 25$  °C).

### 4. Analysis of experimental data

The classical colloid filtration theory (CFT) was used to quantitatively compare the attachment of viruses onto glass beads and clay colloids. The dimensionless collision efficiency,  $\alpha$  (the ratio of the collisions resulting in attachment to the total number of collisions between suspended particles and collector grains), was calculated for each breakthrough curve (Rajagopalan and Tien, 1976):

$$\alpha = -\frac{2d_c \ln(RB)}{3(1-\theta)\eta_0 L} \quad (1)$$

where  $d_c$  [L] is the average collector diameter,  $\eta_0$  [–] is the dimensionless single-collector removal efficiency for favorable deposition (in the absence of double layer interaction energy), and  $RB$  [–] is the ratio of suspended particles  $i$  mass recovery,  $M_{r(i)}$  [–], to the tracer mass recovery,  $M_{r(t)}$  [–], in the outflow:

$$RB = \frac{M_{r(i)}}{M_{r(t)}} \quad (2)$$

where the mass recovery is defined as (Syngouna and Chrysikopoulos, 2011):

$$M_{r(i)}(L) = \frac{\int_0^\infty C_i(L, t) dt}{\int_0^{t_p} C_i(0, t) dt} \quad (3)$$

where  $L$  is the length of the packed column, and  $t_p$  [t] is the duration of tracer or colloid injection (elapsed time period) and  $C_i$  [M/L<sup>3</sup>] is the concentration of suspended particles  $i$ . The total virus concentration,  $C_{Total-v}$  [M/L<sup>3</sup>], was assumed to be equal to the effluent suspended virus concentration,  $C_v$  [M/L<sup>3</sup>], plus the concentration of viruses attached onto suspended clay particles,  $C_{vc}$  [M/L<sup>3</sup>]:

$$C_{Total-v} = C_v + C_{vc} \quad (4)$$

In view of Eqs. (3) and (4), the produced mass,  $M_p$  [–], of  $C_{vc}$  was determined by:

$$M_{p(C_{vc})}(L) = \frac{\int_0^\infty [C_{Total-v}(L, t) - C_v(L, t)] dt}{\int_0^{t_p} C_v(0, t) dt} \quad (5)$$

Finally, the concentration breakthrough data obtained at location  $x = L$  were analyzed by the first normalized temporal moment,  $M_1$ , which defines the mean breakthrough time or average velocity as (James and Chrysikopoulos, 2011):

$$M_{1(i)}(L) = \frac{\int_0^\infty t C_i(L, t) dt}{\int_0^{t_p} C_i(0, t) dt} \quad (6)$$

Note that, the ratio  $M_{1(i)}/M_{1(t)}$  indicates the degree of velocity enhancement of colloid particle  $i$  relative to the conservative tracer. If this ratio is less than one, there exists colloid retardation, and if it is greater than one there exists velocity enhancement of colloid transport (Syngouna and Chrysikopoulos, 2013). In this study, four different normalized temporal moment ratios were calculated,  $M_{1(C_{Total-v})}/M_{1(t)}$ ,  $M_{1(C_v)}/M_{1(t)}$ ,  $M_{1(C_{vc})}/M_{1(t)}$ , and  $M_{1(C_c)}/M_{1(t)}$ , based on the four different effluent concentrations,  $C_{Total-v}$ ,  $C_v$ ,  $C_{vc}$ , and  $C_c$ , respectively. Note that  $C_c$  [M/L<sup>3</sup>], is the effluent suspended clay colloid concentration.

Using the concept of apparent collision efficiency introduced by Walshe et al. (2010), two different apparent collision efficiencies were

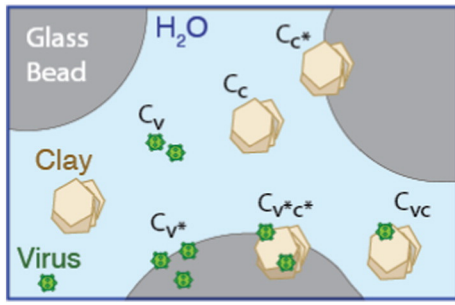


Fig. 1. Schematic illustration of the various concentration in the cotransport experimental study.

calculated. The first collision efficiency,  $\alpha_{\text{Total-v}}$ , is based on  $C_{\text{Total-v}}$  in the effluent and represents the attachment of  $C_v$  onto both glass beads and clay particles attached onto glass beads,  $C_{c^*}$  [M/M]. The second collision efficiency,  $\alpha_v$ , is based on  $C_v$  in the effluent and represents the attachment of both  $C_v$  and  $C_{vc}$  onto glass beads, denoted as  $C_{v^*}$  [M/M] and  $C_{v^*c^*}$  [M/M], respectively, as well as the attachment of  $C_v$  onto both  $C_c$  and  $C_{c^*}$ , denoted as  $C_{vc}$  and  $C_{vc^*}$ , respectively. The six different concentrations accounted for in this study are depicted graphically in Fig. 1.

The collision efficiencies,  $\alpha$ , for MS2 and  $\Phi$ X174 were calculated for the experimental conditions of this study using Eq. (1), where the  $\eta_0$  values were estimated from an existing correlation (Tufenkji and Elimelech, 2004), with the use of the following parameter values: complex Hamaker constant of the interactive media (virus-water-glass beads/clay colloids-water-glass beads)  $A_{123} = 7.5 \times 10^{-21}$  (kg·m<sup>2</sup>/s<sup>2</sup>)

(Murray and Parks, 1978); Boltzman constant  $k_B = 1.38 \times 10^{-23}$  (kg·m<sup>2</sup>)/(s<sup>2</sup>·K); fluid absolute temperature  $T = 298$  K; particle diameter  $d_p = 2.5 \times 10^{-8}$ , and  $2.6 \times 10^{-8}$  m for MS2 and  $\Phi$ X174, respectively; particle density  $\rho_p = 1420$  kg/m<sup>3</sup> for MS2 (Walshe et al., 2010), 1600 kg/m<sup>3</sup> for  $\Phi$ X174 (Feng et al., 2006), and 2200 kg/m<sup>3</sup> for clay colloids (van Olphen and Fripiat, 1979); fluid density  $\rho_f = 999.7$  kg/m<sup>3</sup>; fluid dynamic viscosity  $\mu_f = 8.91 \times 10^{-4}$  kg/(m·s); and acceleration due to gravity  $g = 9.81$  m/s<sup>2</sup>.

For irreversible attachment onto collectors (glass beads), the diffusion-limited virus surface concentration,  $\tilde{C}_{\text{Total-v}}^{\text{dif}}$  [M/L<sup>2</sup>], is given by the following expression (Johnson and Lenhoff, 1996; Dokou et al., 2001):

$$\tilde{C}_{\text{Total-v}}^{\text{dif}} = 2C_{\text{Total-v}} \sqrt{\frac{D_{AB} t_p}{\pi}} \quad (7)$$

where the “tilde” denotes surface concentration [M/L<sup>2</sup>], and  $D_{AB}$  [L<sup>2</sup>/t] is the molecular diffusion coefficient, which can be estimated by the Stokes–Einstein equation (Russel et al., 1989):

$$D_{AB} = \frac{k_B T}{3\pi\mu_B d_p} \quad (8)$$

where the subscript A denotes the solute or colloid particle, and subscript B the solvent (water). Moreover, assuming that the viruses are perfect spheres, the virus diffusion fractional coverage,  $\Omega_{\text{dif}}$  [–], for the cotransport experiments using Eq. (7) was estimated as:

$$\Omega_{\text{dif}} = \tilde{C}_{\text{Total-v}}^{\text{dif}} \left( \frac{A_p}{\rho_p V_p} \right) \quad (9)$$

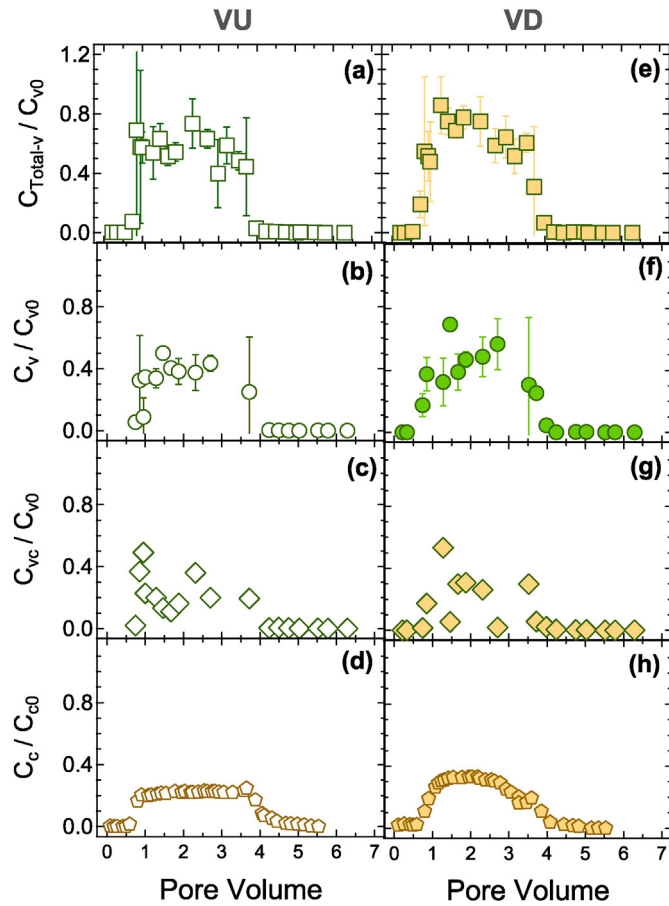


Fig. 2. Experimental data of  $C_{\text{Total-v}}$  (squares),  $C_v$  (circles),  $C_{vc}$  (diamonds), and  $C_c$  (pentagons) for the  $\Phi$ X174 and KGa-1b cotransport experiments with: (a–d) vertical up flow (open symbols), and (e–h) vertical down flow (filled symbols) directions.

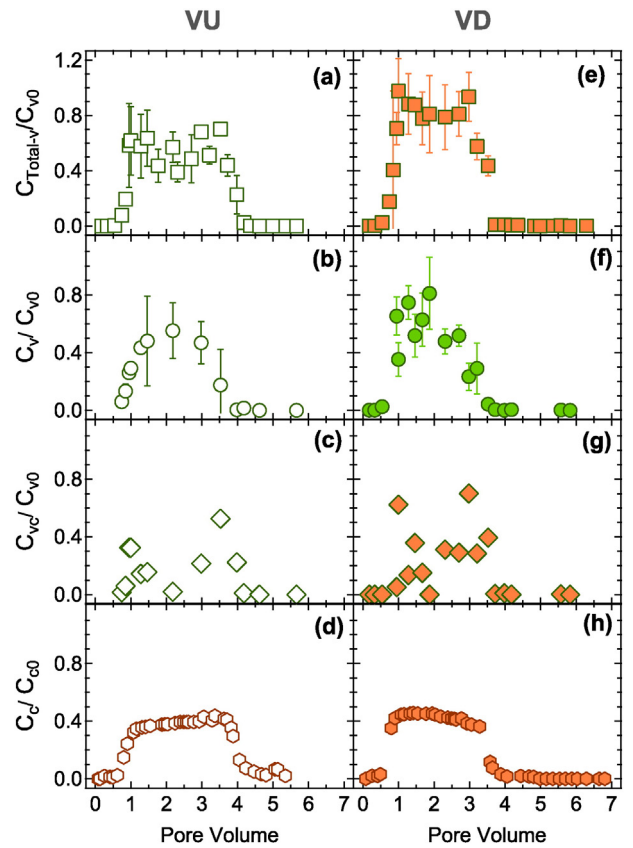


Fig. 3. Experimental data of  $C_{\text{Total-v}}$  (squares),  $C_v$  (circles),  $C_{vc}$  (diamonds), and  $C_c$  (pentagons) for the  $\Phi$ X174 and STx-1b cotransport experiments with: (a–d) vertical up flow (open symbols), and (e–h) vertical down flow (filled symbols) directions.

where  $A_p = \pi d_p^2 / 4 [L^2]$  is the projected particle area, and  $\rho_p V_p [M]$  is the mass of a single particle (where  $V_p = \pi d_p^3 / 6 [L^3]$  is the volume of a single particle).

To evaluate the role of gravity, the fractional coverage of viruses onto collectors (glass beads) was calculated by taking into account only sedimentation. For Stokes flow, the sedimentation velocity of a colloidal particle  $U_s$  is a modified version of the traditional “free particle” settling velocity in static water columns (Russel et al., 1989, p. 395) to “restricted particle” settling in granular porous media under directional flow conditions (Chrysikopoulos and Syngouna, 2014):

$$U_s = -f_s \frac{(\rho_p - \rho_f) d_p^2}{18\mu_f} g_{(i)} \quad (10)$$

where  $f_s$  is the correction factor accounting for particle settling in the presence of the solid matrix of granular porous media with  $f_s \approx 0.9$  when the grains of the granular porous media contribute only to tortuosity and do not provide additional frictional resistance (Wan et al., 1995) and  $g_{(i)}$  accounts for the directional interstitial flow as follows:

$$g_{(i)} = g \sin\beta \quad (11)$$

where  $\beta [^\circ]$  is the angle of the main flow direction with respect to the horizontal x-direction ( $-90^\circ \leq \beta \leq 90^\circ$ ), and  $i$  is the unit vector parallel to the flow (note that for vertical up-flow  $\beta = 90^\circ$  whereas for vertical down-flow  $\beta = -90^\circ$ ).

For irreversible attachment onto glass beads, the sedimentation-limited virus surface concentration,  $\tilde{C}_{\text{Total-v}*}^{\text{sed}} [M/L^2]$ , is given by:

$$\tilde{C}_{\text{Total-v}*}^{\text{sed}} = C_{\text{Total-v}} U_s t_p \quad (12)$$

Thus the virus sedimentation-limited fractional coverage,  $\Omega_{\text{sed}} [-]$  was estimated as follows:

$$\Omega_{\text{sed}} = \tilde{C}_{\text{Total-v}*}^{\text{sed}} \left( \frac{A_p}{M_p} \right) \quad (13)$$

Note that, only diffusion should contribute to coverage of viruses onto the vertical surfaces of the collectors (glass beads), while sedimentation is expected to be significant when the calculated sedimentation value is similar to the diffusion value (Dokou et al., 2001).

## 5. Results and discussion

The normalized cotransport experimental breakthrough data for  $\Phi X174$  and KGa-1b are presented in Fig. 2, and for  $\Phi X174$  and STx-1b in Fig. 3. The corresponding  $M_r$  values, based on  $C_{\text{Total-v}}$  of  $\Phi X174$  in the effluent, as calculated with Eq. (3), were considerably reduced in the presence of clay colloids compared to those obtained in the absence of clay colloids (see Supplementary Fig. S1). This observation is in agreement with the work presented by Syngouna and Chrysikopoulos (2013), and suggests that some clay-bound viruses were retained in

**Table 1**  
Measured and calculated parameter values.

Cotransport experiments								
Flow direction <sup>a</sup>	$\Phi X174$				MS2			
	KGa-1b		STx-1b		KGa-1b		STx-1b	
	VU	VD	VU	VD	VU	VD	VU	VD
Initial concentration								
$C_{v0}$ (PFU/mL)	3400	2767	3850	4817	18,185	9767	9017	9500
$C_{c0}$ (mg/L)	93	80.75	123.92	122.21	70.69	76.98	114.07	92.56
Mass recovery, $M_r$ (%)								
$C_{\text{Total-v}}$	56.27	65.56	60.40	53.48	40.79	54.50	73.21	72.23
$C_v$	35.79	43.57	38.80	31.88	29.90	41.22	51.59	38.11
$C_c$	25.05	27.2	41.19	47.74	36.8	31.41	39.28	42.88
Mass production, $M_p$ (%)								
$C_{vc}$	20.48	21.99	21.40	21.60	10.89	13.28	21.62	34.12
Moment ratios, $M_{1(i)}/M_{1(t)}$								
$C_{\text{Total-v}}$	0.84	0.82	0.89	0.79	0.77	0.78	0.82	0.89
$C_v$	0.86	0.83	0.82	0.82	0.79	0.85	0.81	0.92
$C_{vc}$	0.91	0.79	1.05	1.01	0.80	0.7	0.83	0.93
$C_c$	0.91	0.87	0.94	0.77	0.9	0.85	0.87	0.85
Collision efficiency								
$\alpha_{\text{Total-v}}$	0.11	0.08	0.09	0.11	0.16	0.11	0.05	0.06
$\alpha_v$	0.19	0.15	0.17	0.21	0.21	0.16	0.12	0.17
$\alpha_c$	0.91	0.86	0.34	0.36	0.66	0.76	0.36	0.33
Sedimentation velocity (cm/min) <sup>b</sup>								
viruses	$-1.20E-06$	$1.20E-06$	$-1.20E-06$	$1.20E-06$	$-7.76E-07$	$7.76E-07$	$-7.76E-07$	$7.76E-07$
clays	$-2.52E-03$	$2.52E-03$	$-4.99E-03$	$4.99E-03$	$-2.52E-03$	$2.52E-03$	$-4.99E-03$	$4.99E-03$
Sedimentation limited attachment <sup>c</sup>								
$\tilde{C}_{\text{Total-v}*}^{\text{sed}} [M/L^2]$	-0.19	0.25	-0.37	0.64	-0.32	0.35	-0.74	0.67
Diffusion limited attachment <sup>d</sup>								
$\tilde{C}_{\text{Total-v}*}^{\text{dif}} [M/L^2]$	56.03	73.67	108.95	186.77	146.02	164.01	343.89	307.58
Sedimentation fractional coverage <sup>e</sup>								
$\Omega_{\text{sed}}$ viruses	$-1.20E-10$	$1.57E-10$	$-2.33E-10$	$3.99E-10$	$-1.83E-10$	$2.05E-10$	$-4.31E-10$	$3.85E-10$
Diffusion fractional coverage <sup>f</sup>								
$\Omega_{\text{dif}}$ viruses	$2.97E-10$	$3.91E-10$	$5.78E-10$	$9.92E-10$	$7.17E-10$	$8.05E-10$	$1.69E-09$	$1.51E-09$

<sup>a</sup> VU-vertical up-flow, VD-vertical down-flow.

<sup>b</sup> Evaluated with Eq. (10).

<sup>c</sup> Evaluated with Eq. (12).

<sup>d</sup> Evaluated with Eq. (7).

<sup>e</sup> Evaluated with Eq. (13).

<sup>f</sup> Evaluated with Eq. (9).

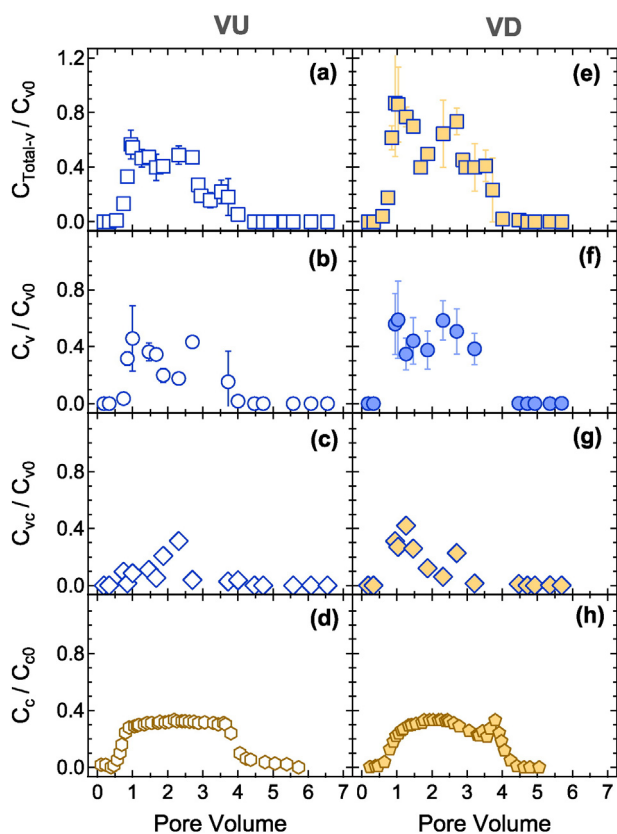


**Fig. 4.** Experimental data of  $C_{\text{Total-v}}$  (squares),  $C_v$  (circles),  $C_{vc}$  (diamonds), and  $C_c$  (pentagons) for the MS2 and KGa-1b cotransport experiments with: (a–d) vertical up flow (open symbols), and (e–h) vertical down flow (filled symbols) directions.

the column due to clay attachment onto glass beads (Vasiliadou and Chrysikopoulos, 2011; Jiang et al., 2007). Furthermore, the ratios  $M_1(C_{\text{Total-v}})/M_1(t)$  for  $\Phi\text{X174}$  (see Table 1) indicated that the transport of  $\Phi\text{X174}$  ( $C_{\text{Total-v}}$ ) was retarded compared to the tracer for both VU and VD flow directions. Actually, KGa-1b and STx-1b were retarded for all  $\Phi\text{X174}$  cotransport cases examined. Moreover, the calculated  $M_1(C_v)/M_1(t)$  ratios for  $\Phi\text{X174}$  indicated that the transport of  $C_v$  was retarded compared to the tracer for both VU and VD flow directions. The same trend was observed for the calculated  $M_1(C_{vc})/M_1(t)$  ratios for  $\Phi\text{X174}$ , except when STx-1b was present, where enhancement of  $C_{vc}$  was observed. As shown in Table 1, for VD flows, KGa-1b hindered the transport of  $\Phi\text{X174}$  ( $[M_1(C_{vc})/M_1(t)] < [M_1(C_{\text{Total-v}})/M_1(t)] < [M_1(C_v)/M_1(t)] < 1$ ). In the presence of STx-1b, for both flow directions examined (VU, VD), the transport of  $\Phi\text{X174}$  was facilitated ( $[M_1(C_{\text{Total-v}})/M_1(t)] < [M_1(C_v)/M_1(t)] < [M_1(C_{vc})/M_1(t)] < 1$  or  $[M_1(C_{vc})/M_1(t)] > [M_1(C_{\text{Total-v}})/M_1(t)] > [M_1(C_v)/M_1(t)] > 1$ ). It is worthy to note that Syngouna and Chrysikopoulos (2013) showed that KGa-1b hindered while STx-1b facilitated the transport of  $\Phi\text{X174}$  in cotransport experiments under horizontal flow with equal flow velocity to the one used in the present study. Despite the highly unfavorable electrostatic conditions of the experiments conducted in this study, significant amount of both clays were retained in the packed columns, suggesting that physical retention was an important filtration mechanism for both  $C_c$  and  $C_{vc}$ .

The normalized cotransport breakthrough data for the two flow directions (VD, VU) are presented for MS2 and KGa-1b in Fig. 4 and for MS2 and STx-1b in Fig. 5. The various  $M_1(C_{\text{Total-v}})/M_1(t)$  for MS2, listed in Table 1, indicated that  $C_{\text{Total-v}}$  of MS2 was retarded compared to the tracer for both flow directions. Note that in the presence of both clays (KGa-1b, STx-1b) for both flow directions examined (VU, VD), the transport of MS2 was facilitated ( $[M_1(C_{\text{Total-v}})/M_1(t)] < [M_1(C_v)/M_1(t)] < [M_1(C_{vc})/M_1(t)] < 1$ ) except in the presence of KGa-1b under VD flow where the transport of MS2 was hindered ( $[M_1(C_{vc})/M_1(t)] < [M_1(C_{\text{Total-v}})/M_1(t)] < [M_1(C_v)/M_1(t)] < 1$ ).

( $t$ )  $< 1$ ) (see Table 1). Therefore, depending on the physicochemical conditions (e.g. chemical nature of clays, surface charge, size and type of virus), colloid particles can facilitate or hinder the transport of viruses in water saturated porous media.

The  $M_r$  values for  $\Phi\text{X174}$ , MS2, KGa-1b and STx-1b, as calculated with Eq. (3), for the two flow directions (VU, VD), are listed in Table 1. Note that the calculated  $M_r$  for both  $\Phi\text{X174}$  and MS2, based on  $C_{\text{Total-v}}$  equals to the  $M_r$  based on  $C_v$  plus the  $M_p$  based on  $C_{vc}$ . The  $M_r$  values based on  $C_v$  and the  $M_p$  values based on  $C_{vc}$  for both  $\Phi\text{X174}$  and MS2, and both flow directions (VU, VD) are presented in Fig. 6. In the presence of both clays (KGa-1b, STx-1b) for both flow directions (VU, VD), the calculated  $M_r$  values based on  $C_v$  of both viruses ( $\Phi\text{X174}$ , MS2), were lower for VU than VD flow. In the presence of STx-1b the opposite was observed. Similar trend was shown for the calculated  $M_r$  values based on  $C_{\text{Total-v}}$  of both viruses ( $\Phi\text{X174}$ , MS2). In the presence of KGa-1b, the calculated  $M_p$  values based on  $C_{vc}$  of MS2, were lower than those in the presence of STx-1b for both flow directions (VU, VD). Comparable  $M_p$  values based on  $C_{vc}$  of  $\Phi\text{X174}$  were observed in the presence of both clays (KGa-1b, STx-1b) for both flow directions (VU, VD). However, in all cases examined, the  $M_p$  values were higher for VD than VU flow, suggesting that the flow direction significantly influences virus deposition onto clays. Note that sedimentation due to gravity can be quite significant for  $C_{vc}$  transport, especially, in studies of VD flow, and can explain the higher  $M_p$  values observed in the effluent. This observation is in agreement with the work by Wan et al. (1995) who investigated the long-term transport of bacteria in the VD flow direction and suggested that sedimentation can explain the presence of bacterial populations in deep subsurface formations. Also, similar  $M_r$  values based on  $C_c$  were observed for both clays (KGa-1b, STx-1b) in the presence of viruses under both flow directions (see Table 1).

The collision efficiency values,  $\alpha_{\text{Total-v}}$ , based on  $C_{\text{Total-v}}$ , and  $\alpha_v$  values based on  $C_v$ , are presented in Fig. 7. Also, the various  $\alpha_{\text{Total-v}}$

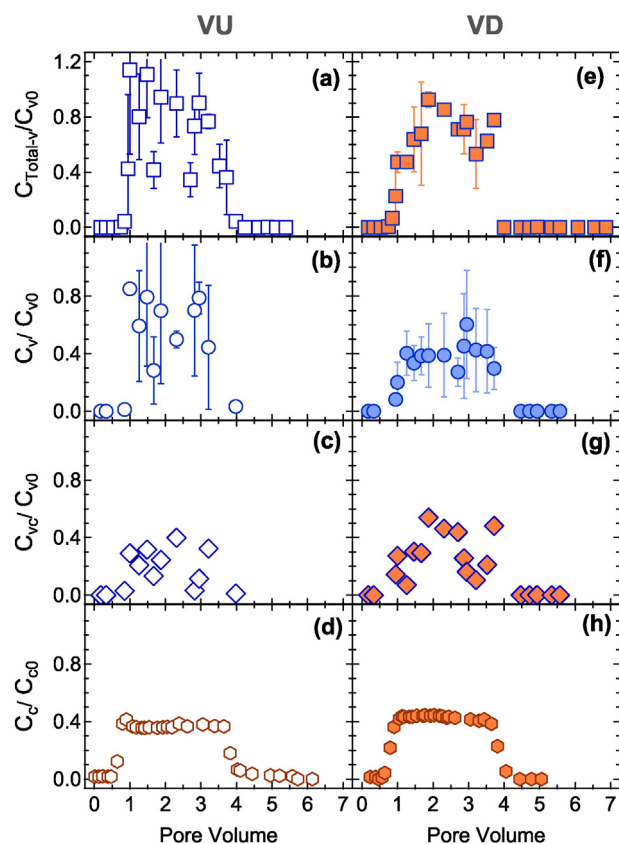


**Fig. 5.** Experimental data of  $C_{\text{Total-v}}$  (squares),  $C_v$  (circles),  $C_{vc}$  (diamonds), and  $C_c$  (pentagons) for the MS2 and STx-1b cotransport experiments with: (a–d) vertical up flow (open symbols), and (e–h) vertical down flow (filled symbols) directions.

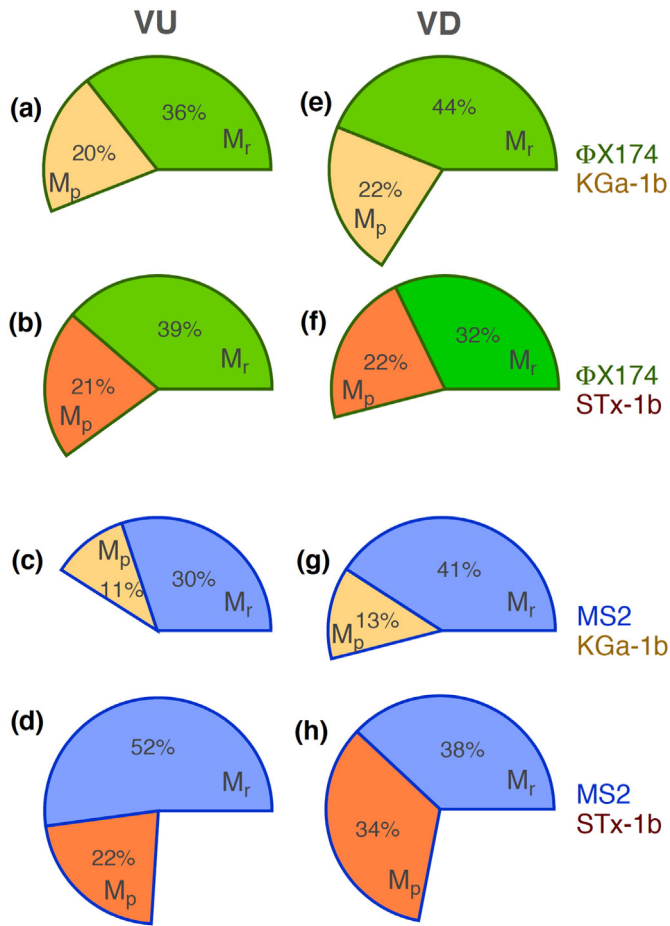


**Fig. 6.** Calculated  $M_r$  values based on  $C_v$  and  $M_p$  values based on  $C_{vc}$  for cotransport of: (a, e)  $\Phi$ X174 with KGA-1b, (b, f)  $\Phi$ X174 with STX-1b, (c, g) MS2 with KGA-1b, and (d, h) MS2 with STX-1b under (a–d) vertical up flow, and (e–h) vertical down flow directions.

and  $\alpha_v$  values were calculated with Eq. (1) for both flow directions, and they are listed in Table 1. The  $\alpha_{Total-v}$  for the cotransport experiments holds information about the attachment of  $C_{Total-v}$  onto glass beads and  $C_{c^*}$ . In the presence of KGA-1b,  $\alpha_{Total-v}$  values were higher in VU than VD flow for both viruses, while in the presence of STX-1b the opposite was observed. Furthermore, the calculated  $\alpha_v$  indicated that the

presence of KGA-1b increased the attachment of virus onto glass beads and clay colloids more than STX-1b under VU flow while STX-1b increased the attachment of both viruses more than KGA-1b under VD flow. Moreover, the higher  $\alpha_v$  values observed for MS2 than  $\Phi$ X174 in the presence KGA-1b may be attributed to the greater affinity of MS2 for KGA-1b particles (Chrysikopoulos and Syngouna, 2012). Worthy to note is that, in agreement with the experimental results of this study, Chrysikopoulos and Syngouna (2012), using extended-DLVO theory to evaluate the attachment of bacteriophages MS2 and  $\Phi$ X174 onto well-crystallized kaolinite (KGA-1b) and montmorillonite (STX-1b) (colloidal fraction  $< 2 \mu\text{m}$ ), reported that Lewis acid–base free energy of interaction,  $\Phi_{AB}(h = h_0)$ , values between viruses and clays at  $h = h_0$  (i.e., at “contact”), were more negative for MS2 than  $\Phi$ X174 interactions with the two clays. Furthermore, it is worthy to note that TEM images shown that the clay particles were non-spherical (Chrysikopoulos and Syngouna, 2012). Thus, assuming that clay particles are spherical may lead to inaccurate predictions of clay colloid fate and transport in porous media (Gallego-Urrea et al., 2014).

The expected coverages  $\Omega_{dif}$  (Eq. (9)) and  $\Omega_{sed}$  (Eq. (13)) and virus surface concentrations  $\tilde{C}_{Total-v^*}^{dif}$  (Eq. (7)) and  $\tilde{C}_{Total-v^*}^{sed}$  (Eq. (12)) of diffusion-limited attachment and attachment by sedimentation, respectively, showed that gravity has smaller effect on  $\tilde{C}_{Total-v^*}^{dif}$  and  $\tilde{C}_{Total-v^*}^{sed}$  of MS2 than of  $\Phi$ X174 (see Table 1). Note that, for  $\Phi$ X174 both  $\tilde{C}_{Total-v^*}^{dif}$  and  $\tilde{C}_{Total-v^*}^{sed}$  were higher under VD than VU flow, while for MS2 no clear trend was observed. Moreover,  $\tilde{C}_{Total-v^*}^{dif}$  was higher for MS2 than  $\Phi$ X174 for all cases examined (see Table 1). Note that,  $C_v$ ,  $C_c$  and  $C_{vc}$  attachment onto glass beads under both flow directions can be affected by the glass bead roughness and local flow conditions created by roughness asperities. Basha and Culligan (2010) conducted experiments under unfavorable attachment conditions and concluded that collector surface asperities significantly affect the filtration process in the VD flow direction, but not in the VU flow direction. Seymour et al. (2013) reported that surface roughness contributes to higher attachment of non-spherical than spherical colloids. Note that Eqs. (7), (9), (12), and (13) for the calculation of virus surface-coverages and virus surface concentrations do not take into account any colloidal interactions (e.g. virus–glass surface, clay–glass surface, virus–clay), which are expected to be significant at the pore-scale. Electrostatic surface heterogeneity of a few nanometers is frequently encountered in colloidal systems (Bendersky et al., 2015). At low ionic strengths, as those in the experiments conducted here, interparticle electrostatic repulsion can enhance the gradient diffusion coefficient (Johnson and Lenhoff, 1996; Raj and

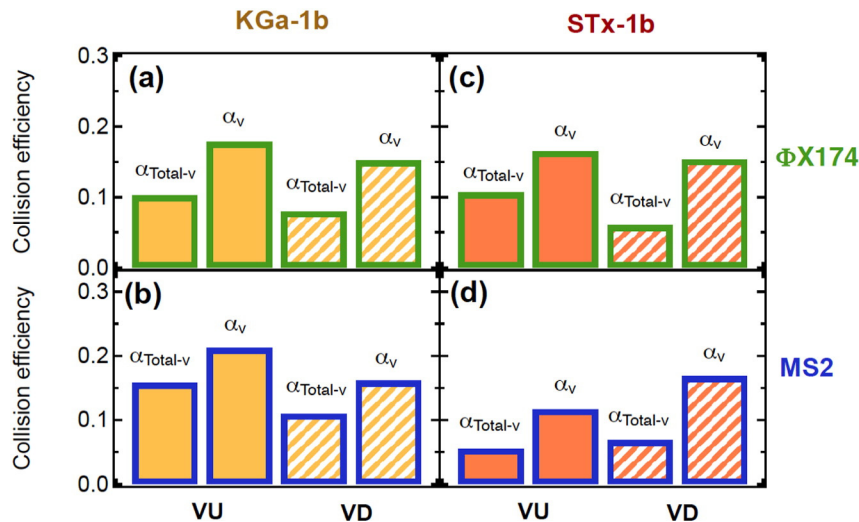


**Fig. 7.** Calculated collision efficiency values,  $\alpha_{Total-v}$ , based on  $C_{Total-v}$ , and  $\alpha_v$  based on  $C_v$ , for cotransport experiments: (a)  $\Phi$ X174 with KGA-1b, (b) MS2 with KGA-1b, (c)  $\Phi$ X174 with STX-1b, and (d) MS2 with STX-1b under vertical up flow (solid bars) and vertical down flow (partially shaded bars) directions.

Flygare, 1974; Anderson et al., 1978). Finally, for the above calculations it was assumed that diffusion and sedimentation occur simultaneously.

## 6. Conclusions

In this study, we have examined the effect of gravity on virus co-transport with clay colloids in water saturated vertical columns under up flow and down flow directions. The results of this study indicated that KGa-1b hindered the transport of  $\Phi$ X174 under VD flow, while STx-1b facilitated the transport of  $\Phi$ X174 under both VU and VD flows. Moreover, KGa-1b and STx-1b facilitated the transport of MS2 in most of the cases examined, except for the case where KGa-1b was present under VD flow. Note that, in the presence of KGa-1b, estimated mass recovery values for both viruses were higher for VD than VU flow, while in the presence of STx-1b the opposite was observed. This could be attributed to higher affinity of both viruses for KGa-1b than STx-1b, and to lower retention of virus-KGa-1b complexes by the packed column. However, in all cases examined, the produced mass of viruses attached onto suspended clay particles were higher for VD than VU flow, suggesting that VD flow enables viruses attached onto clays to penetrate subsurface formations and thus to travel long distances within aquifers, which is an important public health issue. Note that virus attachment onto clays does not invariably lead to virus inactivation, and virus-clay complexes may be as infectious as unattached viruses. Moreover, theoretical calculations showed that gravity has a smaller effect on both diffusion-limited and sedimentation-limited attachment of MS2 onto glass beads than that of  $\Phi$ X174.

## Acknowledgments

This research has been co-financed by the European Union (European Social Fund—ESF) and Greek national funds through the Operational program “Education and Lifelong Learning” of the National Strategic Reference Framework (NSRF)—Research Funding Program: Aristeia I (Code 1185).

## Appendix A. Supplementary data

Supplementary data to this article can be found online at <http://dx.doi.org/10.1016/j.scitotenv.2015.12.091>.

## References

- Adams, M.H., 1959. Bacteriophages. Interscience, New York, N.Y., pp. 450–454.
- Anders, R., Chrysikopoulos, C.V., 2006. Evaluation of the factors controlling the time-dependent inactivation rate coefficients of bacteriophage MS2 and PRD1. *Environ. Sci. Technol.* 40 (10), 3237–3242.
- Anders, R., Chrysikopoulos, C.V., 2009. Transport of viruses through saturated and unsaturated columns packed with sand. *Transp Porous Media* 76 (1), 121–138.
- Anderson, J.L., Rauh, F., Morales, A., 1978. Particle diffusion as a function of concentration and ionic strength. *J. Phys. Chem.* 82 (5), 608–616.
- Basha, H.A., Culligan, P.J., 2010. Modeling particle transport in downward and upward flows. *Water Resour. Res.* 46, W07518. <http://dx.doi.org/10.1029/2009WR008133>.
- Bellou, M., Syngouna, V.I., Tselipi, M.A., Kokkinos, P.A., Paparrodopoulos, S.C., Chrysikopoulos, C.V., Vantarakis, A., 2015. Interaction of human adenovirus and coliphages with kaolinite and bentonite. *Sci. Total Environ.* 517, 86–95. <http://dx.doi.org/10.1016/j.scitotenv.2015.02.036>.
- Bendersky, M., Santore, M.M., Davis, J.M., 2015. Statistically-based DLVO approach to the dynamic interaction of colloidal microparticles with topographically and chemically heterogeneous collectors. *J. Colloid Interface Sci.* 449, 443–451.
- Bradford, S.A., Torkzaban, S., 2012. Colloid adhesive parameters for chemically heterogeneous porous media. *Langmuir* 28, 13643–13651.
- Bradford, S.A., Torkzaban, S., 2013. Colloid interaction energies for physically and chemically heterogeneous porous media. *Langmuir* 29, 3668–3676.
- Bradford, S.A., Simunek, J., Walker, S.L., 2006. Transport and straining of *E. coli* O157:H7 in saturated porous media. *Water Resour. Res.* 42, W12S12. <http://dx.doi.org/10.1029/2005WR004805>.
- Chrysikopoulos, C.V., Aravantinou, A.F., 2012. Virus inactivation in the presence of quartz sand under static and dynamic batch conditions at different temperatures. *J. Hazard. Mater.* 233–234, 148–157.
- Chrysikopoulos, C.V., Katzourakis, V.E., 2015. Colloid particle size-dependent dispersivity. *Water Resour. Res.* 51, 4668–4683. <http://dx.doi.org/10.1002/2014WR016094>.
- Chrysikopoulos, C.V., Sim, Y., 1996. One-dimensional virus transport in homogeneous porous media with time-dependent distribution coefficient. *J. Hydrol.* 185, 199–219.
- Chrysikopoulos, C.V., Syngouna, V.I., 2012. Attachment of bacteriophages MS2 and  $\Phi$ X174 onto kaolinite and montmorillonite: extended DLVO interactions. *Colloids Surf., B* 92, 74–83.
- Chrysikopoulos, C.V., Syngouna, V.I., 2014. Effect of gravity on colloid transport through water-saturated columns packed with glass beads: modeling and experiments. *Environ. Sci. Technol.* 48, 6805–6813. <http://dx.doi.org/10.1021/es501295v>.
- Chrysikopoulos, C.V., Masciopinto, C., La Mantia, R., Manariotis, I.D., 2010. Removal of biocolloids suspended in reclaimed wastewater by injection in a fractured aquifer model. *Environ. Sci. Technol.* 44 (3), 971–977.
- Chrysikopoulos, C.V., Syngouna, V.I., Vasiliadou, I.A., Katzourakis, V.E., 2012. Transport of *Pseudomonas putida* in a three-dimensional bench scale experimental aquifer. *Transp. Porous Media* 94, 617–642. <http://dx.doi.org/10.1007/s11242-012-0015-z>.
- Degeldre, C., Pfeiffer, H.R., Alexander, W., Wernli, B., Brutsch, R., 1996. Colloidal properties in granitic groundwater systems. *Appl. Geochem.* 11, 677–695.
- DeNovio, N.M., Saiers, J.E., Ryan, J.N., 2004. Colloid movement in unsaturated porous media: recent advances and future directions. *Vadose Zone J.* 3, 338–351.
- Dokou, E., Barteau, M.A., Wagner, N.J., Lenhoff, A.M., 2001. Effect of gravity on colloidal deposition studied by atomic force microscopy. *J. Colloid Interface Sci.* 240 (1), 9–16. <http://dx.doi.org/10.1006/jcis.2001.7626>.
- Feng, H., Yu, Z., Chu, P.K., 2006. Ion implantation of organisms. *Materials Sci. Eng. R: Reports* 54 (3–4), 49–120.
- Gallego-Urrea, J.A., Hammes, J., Cornelis, G., Hasselov, M., 2014. Multimethod 3D characterization of natural plate-like nanoparticles: shape effects on equivalent size measurements. *J. Nanopart. Res.* 16 (5), 2382–2383. <http://dx.doi.org/10.1007/s11051-014-2383-5>.
- Gantzer, C., Maul, A., Audic, J.M., Schwartzbrod, L., 1998. Detection of infectious enteroviruses, enterovirus genomes, somatic coliphages, and *Bacteroides fragilis* phages in treated wastewater. *Appl. Environ. Microbiol.* 64, 4307–4312.
- Gao, B., Saiers, J.E., Ryan, J.N., 2004. Deposition and mobilization of clay colloids in unsaturated porous media. *Water Resour. Res.* 40, W08602. <http://dx.doi.org/10.1029/2004WR003189>.
- James, S.C., Chrysikopoulos, C.V., 2011. Monodisperse and polydisperse colloid transport in water-saturated fractures with various orientations: gravity effects. *Adv. Water Resour.* 34 (10), 1249–1255.
- Jiang, D., Huang, Q., Cai, P., Rong, X., Chen, W., 2007. Adsorption of *Pseudomonas putida* on clay minerals and iron oxide. *Colloids Surf. B* 54 (2), 217–221.
- Jin, Y., Flury, M., 2002. Fate and transport of viruses in porous media. *Adv. Agron.* 77, 39–102.
- Johnson, C.A., Lenhoff, A.M., 1996. Adsorption of charged latex particles on mica studied by atomic force microscopy. *J. Colloid Interface Sci.* 179 (2), 587–599.
- Katzourakis, V.E., Chrysikopoulos, C.V., 2014. Mathematical modeling of colloid and virus cotransport in porous media: application to experimental data. *Adv. Water Resour.* 68, 62–73. <http://dx.doi.org/10.1016/j.advwatres.2014.03.001>.
- Katzourakis, V.E., Chrysikopoulos, C.V., 2015. Modeling dense-colloid and virus cotransport in three-dimensional porous media. *J. Contam. Hydrol.* 181, 102–113. <http://dx.doi.org/10.1016/j.jconhyd.2015.05.010>, 2015.
- Kim, H.N., Bradford, S.A., Walker, S.L., 2009. *Escherichia coli* O157:H7 transport in saturated porous media: role of solution chemistry and surface macromolecules. *Environ. Sci. Technol.* 43 (12), 4340–4347.
- Kokkinos, P., Syngouna, V.I., Tselipi, M.A., Bellou, M., Chrysikopoulos, C.V., Vantarakis, A., 2015. Transport of human adenoviruses in water saturated laboratory columns. *Food Environ. Virol.* 7, 122–131. <http://dx.doi.org/10.1007/s12560-014-9179-8>.
- Kretzschmar, R., Borkovec, M., Grolimund, D., Elimelech, M., 1999. Mobile subsurface colloids and their role in contaminant transport. *Adv. Agron.* 66, 121–194.
- Ma, H., Johnson, W.P., 2010. Colloid retention in porous media of various porosities: predictions by the hemispheres-in-cell model. *Langmuir* 26 (3), 1680–1687.
- Ma, H., Pedel, J., Fife, P., Johnson, W.P., 2009. Hemispheres-in-cell geometry to predict colloid deposition in porous media. *Environ. Sci. Technol.* 43 (22), 8573–8579.
- Mitropoulou, P.N., Syngouna, V.I., Chrysikopoulos, C.V., 2013. Transport of colloids in unsaturated packed columns: role of ionic strength and sand grain size. *Chem. Eng. J.* 232, 237–248. <http://dx.doi.org/10.1016/j.cej.2013.07.093>.
- Moulin, V., Ouzounian, G., 1992. Role of colloids and humic substances in the transport of radio-elements through the geosphere. *Appl. Geochem.* 511, 179–186.
- Murray, J.P., Parks, G.A., 1978. Particulates in water: characterization, fate, effects and removal. In: Kavanaugh, M.C., Leckie, J.O. (Eds.), *Adv. Chem. Ser.* 189. American Chemical Society, Washington, DC.
- Pruett, R.J., Webb, H.L., 1993. Sampling and analysis of KGa-1b well-crystallized kaolin source clay. *Clays and Clay Minerals* 41 (4), 514–519.
- Raj, T., Flygare, W.H., 1974. Diffusion studies on bovine serum albumin by quasi elastic light scattering. *Biochem.* 13 (16), 3336–3340.
- Rajagopalan, R., Tien, C., 1976. Trajectory analysis of deep-bed filtration with the sphere-in-cell porous media model. *AIChE J.* 22 (3), 523–533.
- Rong, X., Huang, Q., He, X., Chen, H., Cai, P., Liang, W., 2008. Interaction of *Pseudomonas putida* with kaolinite and montmorillonite: a combination study by equilibrium adsorption, ITC, SEM and FTIR. *Colloids Surf., B* 64 (1), 49–55.
- Russel, W.B., Saville, D.A., Schowalter, W.R., 1989. *Colloidal Dispersions*. Cambridge University Press, Cambridge, UK 525 pp.
- Ryan, J.N., Harvey, R.W., Metge, D., Elimelech, M., Navigato, T., Pieper, A.P., 2002. Field and laboratory investigations of inactivation of viruses (PRD1 and MS2) adsorbed to iron oxide-coated quartz sand. *Environ. Sci. Technol.* 36, 2403–2413.
- Sanders, R.L., Washton, N.M., Mueller, K.T., 2010. Measurement of the reactive surface area of clay minerals using solid-state NMR studies of a probe molecule. *J. Phys. Chem. C* 114 (12), 5491–5498.
- Schijven, J.F., Hassanizadeh, S.M., 2000. Removal of viruses by soil passage: overview of modeling, processes, and parameters. *Crit. Rev. Environ. Sci. Technol.* 30, 49–127.

- Schjiven, J.F., Hoogenboezem, W., Hassanizadeh, S.M., 1999. Modelling removal of bacteriophages MS2 and PRD1 by dune recharge at castricum. Netherlands. *Water Resour. Res.* 35 (4), 1101–1111.
- Seetha, N., Kumar, M.S.M., Hassanizadeh, S.M., 2015. Modeling the co-transport of viruses and colloids in unsaturated porous media. *J. Contam. Hydrol.* 181, 82–101.
- Sen, T.K., 2011. Processes in pathogenic biocolloidal contaminants transport in saturated and unsaturated porous media: a review. *Water Air Soil Pollut.* 216, 239–256.
- Seymour, M.B., Chen, G., Su, C., Li, Y., 2013. Transport and retention of colloids in porous media: does shape really matter? *Environ. Sci. Technol.* 47, 8391–8398.
- Shen, C., Lazouskaya, V., Zhang, H., Wang, F., Li, B., Jin, Y., Huang, Y., 2012. Theoretical and experimental investigation of detachment of colloids from rough collector surfaces. *Colloids Surf., A* 410, 98–110.
- Silliman, S.E., Dunlap, R., Fletcher, M., Schneegurt, M.A., 2001. Bacterial transport in heterogeneous porous media: observations from laboratory experiments. *Water Resour. Res.* 37 (11), 2699–2707.
- Sim, Y., Chrysikopoulos, C.V., 1996. One-dimensional virus transport in porous media with time-dependent inactivation rate coefficients. *Water Resour. Res.* 32 (8), 2607–2611.
- Sim, Y., Chrysikopoulos, C.V., 1999. Analytical models for virus adsorption and inactivation in unsaturated porous media. *Colloids Surf. A* 155, 189–197.
- Snowdon, J.A., Cliver, D.O., Hurst, C.J., 1989. Coliphages as indicators of human enteric viruses in groundwater. *Critical Rev. Environ. Control* 19 (3), 231–249.
- Syngouna, V.I., Chrysikopoulos, C.V., 2011. Transport of biocolloids in water saturated columns packed with sand: effect of grain size and pore water velocity. *J. Contam. Hydrol.* 126 (3–4), 301–314.
- Syngouna, V.I., Chrysikopoulos, C.V., 2013. Cotransport of clay colloids and viruses in water saturated porous media. *Colloids Surf., A* 416, 56–65.
- Syngouna, V.I., Chrysikopoulos, C.V., 2015. Experimental investigation of virus and clay particles cotransport in partially saturated columns packed with glass beads. *J. Colloid Interface Sci.* 440, 140–150.
- Tong, M., Johnson, W.P., 2006. Excess colloid retention in porous media as a function of colloid size, fluid velocity, and grain angularity. *Environ. Sci. Technol.* 40 (24), 7725–7731.
- Tong, M., Johnson, W.P., 2007. Colloid population heterogeneity drives hyperexponential deviation from classic filtration theory. *Environ. Sci. Technol.* 41 (2), 493–499.
- Tong, M., Ma, H., Johnson, W.P., 2008. Funneling of flow into grain-to-grain contacts drives colloid–colloid aggregation in the presence of an energy barrier. *Environ. Sci. Technol.* 42 (8), 2826–2832.
- Torkzaban, S., Bradford, S.A., Walker, S.L., 2007. Resolving the coupled effects of hydrodynamics and DLVO forces on colloid attachment in porous media. *Langmuir* 33, 9652–9660.
- Torkzaban, S., Bradford, S.A., Vanderzalm, J.L., Patterson, B.M., Harris, B., Prommer, H., 2015. Colloid release and clogging in porous media: effects of solution ionic strength and flow velocity. *J. Contam. Hydrol.* 181, 161–171.
- Tosco, T., Tiraferrri, A., Sethi, R., 2009. Ionic strength dependent transport of microparticles in saturated porous media: modeling mobilization and immobilization phenomena under transient chemical conditions. *Environ. Sci. Technol.* 43, 4425–4431.
- Tufenkji, N., Elimelech, M., 2004. Correlation equation for predicting single-collector efficiency in physicochemical filtration in saturated porous media. *Environ. Sci. Technol.* 38 (2), 529–536.
- Van Olphen, H., Fripiat, J.J., *Data Handbook for Clay Minerals and Other Non-metallic Minerals*. Pergamon Press, Oxford, England, 1979 346 pp.
- Vasiliadou, I.A., Chrysikopoulos, C.V., 2011. Cotransport of *Pseudomonas putida* and kaolinite particles through water saturated porous media. *Water Resour. Res.* 47, W02543. <http://dx.doi.org/10.1029/2010WR009560>.
- Walshe, G.E., Pang, L., Flury, M., Close, M.E., Flintoft, M., 2010. Effects of pH, ionic strength, dissolved organic matter, and flow rate on the cotransport of MS2 bacteriophages with kaolinite in gravel aquifer media. *Water Res.* 44 (4), 1255–1269.
- Wan, J., Tokunaga, T., Tsang, C., 1995. Bacterial sedimentation through a porous medium. *Water Resour. Res.* 31 (7), 1627–1636.
- Xu, S., Gao, B., Saiers, J.E., 2006. Straining of colloidal particles in saturated porous media. *Water Resour. Res.* 42, W12S16. <http://dx.doi.org/10.1029/2006WR004948>.
- Yamagishi, H., Ozeki, H., 1972. Comparative study of thermal inactivation of phage  $\phi 80$  and Lambda. *Virology* 48, 316–322.
- Yates, M.V., Yates, S.R., 1988. Modeling microbial fate in the subsurface environment. *Crit. Rev. Environ. Control.* 17 (4), 307–344.
- Yoon, J.K., Germaine, J.T., Culligan, P.J., 2006. Visualization of particle behavior within a porous medium: mechanisms for particle filtration and retardation during downward transport. *Water Resour. Res.* 42, W06417. <http://dx.doi.org/10.1029/2004WR003660>.
- Zhuang, J., Jin, Y., 2003. Virus retention and transport through Al-coated sand columns: effects of ionic strength and composition. *J. Contam. Hydrol.* 60 (3–4), 193–209.